

DoPa: A Comprehensive CNN Detection Methodology against Physical Adversarial Attacks

Zirui Xu, Fuxun Yu, Xiang Chen
George Mason University, Fairfax, Virginia
{z xu21, fyu2, xchen26}@gmu.edu

ABSTRACT

Recently, Convolutional Neural Networks (CNNs) demonstrate a considerable vulnerability to adversarial attacks, which can be easily misled by adversarial perturbations. With more aggressive methods proposed, adversarial attacks can be also applied to the physical world, causing practical issues to various CNN powered applications. To secure CNNs, adversarial attack detection is considered as the most critical approach. However, most existing works focus on superficial patterns and merely search a particular method to differentiate the adversarial inputs and natural inputs, ignoring the analysis of CNN inner vulnerability. Therefore, they can only target to specific physical adversarial attacks, lacking expected versatility to different attacks. To address this issue, we propose *DoPa* – a comprehensive CNN detection methodology for various physical adversarial attacks. By interpreting the CNN’s vulnerability, we find that non-semantic adversarial perturbations can activate CNN with significantly abnormal activations and even overwhelm other semantic input patterns’ activations. Therefore, we add a self-verification stage to analyze the semantics of distinguished activation patterns, which improves the CNN recognition process. We apply such a detection methodology into both image and audio CNN recognition scenarios. Experiments show that *DoPa* can achieve an average rate of 90% success for image attack detection and 92% success for audio attack detection.

Announcement:[The original DoPa draft on arXiv was modified and submitted to a conference already, while this short abstract was submitted only for a presentation at the KDD 2019 AIoT Workshop.]

KEYWORDS

Physical Adversarial Attack, Neural Network, Detection

1 INTRODUCTION

In the past few years, Convolutional Neural Networks (CNNs) have been widely applied in various cognitive applications, such as image classification [24, 29] and speech recognition [7, 8], *etc.* Although effective and popular, CNN powered applications are facing a critical challenge – adversarial attacks. By injecting particular perturbations into input data, adversarial attacks can mislead CNN recognition results. With aggressive methods proposed, adversarial perturbations can be concentrated into a small area and attached to the real objects, which easily threaten the CNN recognition systems in the physical world. Recently, physical adversarial attacks becomes severe with increasing CNN based applications [3, 15].

Many research works have been proposed to detect the physical adversarial attacks [13, 18, 20, 26]. However, most of them neglect analysis of CNN’s intrinsic vulnerability to adversarial attacks. Instead, either they merely focus on examining the superficial input patterns to differentiate the adversarial inputs and natural

inputs or they simply adopt multiple CNNs to conduct the cross-verification [26, 27]. Therefore, all these methods have a certain drawback: they can only detect specific physical adversarial attacks, lacking versatility to different physical adversarial attacks.

In this paper, we propose *DoPa*, a comprehensive detection methodology for physical adversarial attacks. By interpreting CNN’s vulnerability, we reveal that the CNN’s decision-making process lacks necessary qualitative semantics distinguishing ability: the non-semantic input patterns can dramatically activate CNN and overwhelm other semantic input patterns. We improve the CNN recognition process by adding a self-verification stage to verify the semantics of distinguished activation patterns during CNN inference. For each input image, the verification stage will locate the significant activation sources and calculate the input semantic inconsistency with the expected semantic patterns according to the prediction result. Once the inconsistency exceeds a pre-defined threshold, CNN will predict the input is an adversarial example.

Specifically, we have the following contributions in this work:

- By interpreting CNN’s vulnerability, we discover that the non-semantic input patterns can significantly activate CNN and overwhelm other semantic input patterns.
- We propose a self-verification stage to analyze and detect the abnormal activation patterns’ semantics. Specifically, we develop the inconsistency between the local input patterns that cause the distinguished activations and the synthesized patterns with expected semantics.
- We apply the proposed self-verification detection methodology into two scenarios for image and audio applications.

Experiments show that our method can achieve average 90% and 92% detection successful rates for image physical adversarial attacks and audio physical adversarial attacks, respectively.

2 BACKGROUND AND RELATED WORKS

2.1 Physical Adversarial Attacks

The adversarial attack started to arouse researchers’ general concern with adversarial examples, which were first introduced by [12]. The adversarial examples were designed to project prediction errors into input space to generate noises, which can perturb digital input data (*e.g.*, images and audio clips) and manipulate prediction results. Since then, various adversarial attacks were proposed, such as L-BFGS [22], FGSM [12], CW [6], *etc.* Most of them share a similar mechanism, which tries to cause the most error increment within model activation and regulate the noises within the input space.

Recently, such an attack approach was also brought from the algorithm domain into the physical world, which were referred as physical adversarial attacks. [11] first leveraged a masking method to concentrate adversarial perturbations into a small area and implement attacks on real traffic signs with taped graffiti. [5] then

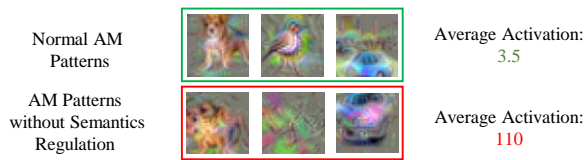


Figure 1: Visualized Neuron’s Input Pattern by Activation Maximization Visualization

extended the scope of physical attacks with adversarial patches. With more aggressive image patterns than taped graffiti, these patches could be attached to physical objects arbitrarily and have a certain degree of model transferability.

Beyond aforementioned image scenarios, some physical adversarial attacks also have been proposed to audios. Yakura *et al.* [25] proposed an audio physical adversarial attack that can still be effective after playback and recording in the physical world. [25] generated audio adversarial command in a normal song which can be played through the air.

Compared to the noise based adversarial attacks, these physical adversarial attacks reduce the attack difficulty and further impair the practicality and reliability of deep learning technologies.

2.2 Image and Audio physical Adversarial Attack Detection

There are several works have been proposed to detect such physical adversarial attacks in the image and speech recognition process [13, 18, 26, 27]. Hayes *et al.* proposed a physical image adversarial attack detection method by applying image erosion and dilation [13]. With these image processing methods, they successfully detect the localization of adversarial noises in input images. Zeng *et al.* leveraged multiple Automatic Speech Recognition (ASR) systems to detect audio physical adversarial attack according to the cross-verification methodology [27]. Yang *et al.* proposed an audio adversarial attack detection method by exploring the temporal dependency existing in audio adversarial attacks [26].

Although having effective detection performance for physical adversarial attacks, these methods are designed for solving specific adversarial attack which are not integrated for different physical adversarial attack situations. Therefore, we develop a comprehensive defection methodology to address the above issue.

3 CNN VULNERABILITY ANALYSIS FOR PHYSICAL ADVERSARIAL ATTACKS

In this section, we first interpret the CNN vulnerability by analyzing input patterns’ semantics with the activation maximization visualization [10]. Based on the semantics analysis, we identify adversarial attack patches as non-semantic input patterns with abnormally distinguished activations. Specifically, to evaluate semantics, we propose metrics that can measure the inconsistencies between the local input patterns that cause the distinguished activations and the synthesized patterns with expected semantics. Based on the inconsistency analysis, we further propose a detection methodology by adding a self-verification stage into CNN inference.

3.1 CNN Vulnerability Interpretation

Interpretation and Assumption: In a typical image or audio recognition process, CNN extracts features from the original input data and gradually derive a prediction result. However, when injecting physical adversarial perturbations into the original data,

CNN will be misled to a wrong prediction result. To better interpret the CNN vulnerability, we first use a typical image physical adversarial attack – adversarial patch attack as an example. In Fig. ??, by comparing with the original input, we find an adversarial patch usually has no constraints in color/shape, *etc.* Such patches usually sacrifice the semantic structures so as to cause significant abnormal activations and overwhelm other input patterns’ activations. *Therefore, we make an assumption that CNN lacks qualitative semantics distinguishing ability which can be activated by the non-semantic adversarial patch during inference.*

Assumption Verification: To verify such an assumption, we need to investigate the semantic of each neuron in CNN. According to our assumption, the non-semantic input patterns will lead to abnormal activations while the semantic input patterns generate normal activations. We adopt a visualized CNN semantic analysis method – Activation Maximization Visualization (AM) [10]. By generating a pattern $V(N_i^l)$ to maximize the i th neuron N_i^l in the layer of l , we can visualize each neuron’s most activated input. Mathematically, this process can be formulated as:

$$V(N_i^l) = \arg \max_x A_i^l(X), \quad X \leftarrow X + \eta \cdot \frac{\partial A_i^l(X)}{\partial X}, \quad (1)$$

where, $A_i^l(X)$ is the activation of N_i^l from an input image X , η is the gradient ascent step size.

Fig. 1 shows the visualized neurons’ semantic input patterns by using AM. As the traditional AM method is designed for semantics interpretation, many feature regulations and hand-engineered natural image references are involved in generating interpretable visualization patterns. Therefore we can get three AM patterns with an average activation magnitude value of 3.5 in Fig. 1 (a). The objects in the three patterns indicate they have clear semantics. However, when we remove these semantics regulations in the AM process, we obtain three different visualized patterns as shown in Fig. 1 (b). We can find that these three patterns are non-semantic, but they have significant abnormal activations with an average magnitude value of 110. This phenomenon can prove our assumption that CNN neurons lack semantics distinguishing ability and can be significantly activated by **non-semantic** inputs patterns.

3.2 Inconsistency Metrics for Input Semantic and Prediction Activation

Inconsistency Identification: To identify the non-semantic input patterns for the attack detection, we examine its impacts during CNN inference by comparing the natural image recognition with the physical adversarial attacks.

Fig. 2 shows a typical adversarial patch based physical attack. The patterns in the left circles are the primary activation sources from the input images, and the bars on the right are the neurons’ activations in the last convolutional layer. From the aspect of input patterns, we find a significant difference between the adversarial patch and primary activation source on the original image, which is referred as **input semantic inconsistency**; From the aspect of prediction activation magnitudes, we observe another difference between the adversarial input and the original input, which is referred as **prediction activation inconsistency**.

Inconsistency Metrics: We further define two metrics to indicate above two inconsistencies’ degrees.

1) Input Semantic Inconsistency Metric. This metric measures the input semantic inconsistency between the non-semantic adversarial patches and the semantic local input patterns from the natural image. It can be defined as follows:

$$D(P_{pra}, P_{ori}) = 1 - S(P_{pra}, P_{ori}), P_{pra} \leftarrow \Phi: A_i^l(p), P_{ori} \leftarrow \Phi: A_i^l(o), \quad (2)$$

where P_{pra} and P_{ori} represent the input patterns from the adversarial input and the original input. $\Phi: A_i^l(p)$ and $\Phi: A_i^l(o)$ represent the set of neurons' activations produced by adversarial patch and the original input, respectively. \mathfrak{X} maps neurons' activations to the primary local input patterns. S represents a similarity metric.

2) Prediction Activation Inconsistency Metric. The second inconsistency is in the activation level, which reveals the activations' magnitude distribution inconsistency in the last convolutional layer between the adversarial input and the original input. We also use a similar metric to measure it as follows:

$$D(f_{pra}, f_{ori}) = 1 - S(f_{pra}, f_{ori}), f_{pra} \sim \Phi: A_i^l(p), f_{ori} \sim \Phi: A_i^l(o), \quad (3)$$

where f_{pra} and f_{ori} represent the magnitude distribution of activations in the last convolutional layer generated by the adversarial input and the original input data.

For the above two inconsistency metrics, we can easily obtain P_{pra} and f_{pra} since they come from the input data. However, P_{ori} and f_{ori} are not easily to get because of the variety of the natural input data. Therefore, we need to synthesize the standard input data which can provide the semantic input patterns and activation magnitude distribution. The synthesized input data for each prediction class can be obtained from a standard dataset. By feeding CNN with a certain number of input from the standard dataset, we can record the average activation magnitude distribution in last convolutional layer. Moreover, we can locate the primary semantic input patterns for each prediction class.

3.3 Inconsistency for Physical Adversarial Attack Detection

The proposed two inconsistencies demonstrate the difference between physical adversarial attacks and natural image recognition in terms of input patterns and prediction activations, we can leverage the two inconsistency metrics to measure the inconsistencies and further detect the physical adversarial attacks. Specifically, when the measured inconsistency values exceed the given thresholds, we consider the input as an adversarial input.

Since the two metrics can be easily calculated during CNN inference, we integrate them as a **self-verification** stage in the CNN decision-making process. During the inference, CNN leverages this self-verification stage to measure the inconsistencies and further achieve adversarial input verification.

We apply such **detection** methodology for both image and audio applications in Section 4 and Section 5.

4 IMAGE PHYSICAL ADVERSARIAL ATTACK DETECTION

In this section, we will describe how to leverage our proposed methodology to detect the image physical adversarial attacks based on the **input semantic inconsistency** in input pattern level.

Inconsistency Derivation: First, by using Class Activation Mapping (CAM) [28], we locate the primary activation source from the input image. Assume the k^{th} activation in the last convolutional layer is $A_k(x, y)$ and its spatial location is (x, y) , we can compute a

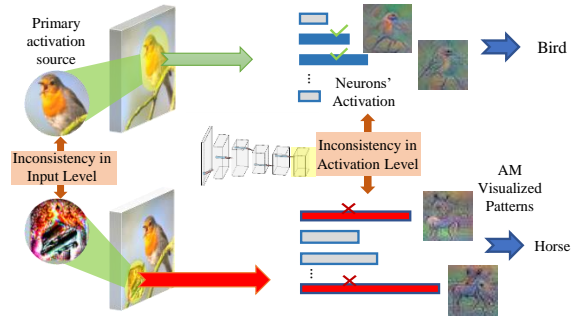


Figure 2: Image Adversarial Patch Attack weight sum of all activations at the (x, y) in the last convolutional layer as:

$$A_T(x, y) = \sum_K A_k(x, y), \quad (4)$$

where K is the total number of activations in the last convolutional layer. A larger value of $A_T(x, y)$ represents the activation source in the input image at the corresponding spatial location (x, y) is more important for classification result.

A specific input semantic inconsistency metric is further required for achieving CNN self-verification. Since the input adversarial patch contains more high-frequency information than the natural semantic input patterns, we differentiate them from the aspect of frequency. 2D Fast Fourier Transform (2D-FFT) [2] is introduced to concentrate the low-frequency component together in frequency domain. Furthermore, we convert the frequency-domain pattern to a binary pattern with an adaptive threshold. For binary patterns, we can observe the significant difference between adversarial input and semantic synthesized input. Therefore, we replace $S(I_{pra}, I_{ori})$ as Jaccard Similarity Coefficient (JSC) [19] and propose our image adversarial attack inconsistency metric as:

$$D(P_{pra}, P_{exp}) = 1 - JSC(P_{pra}, P_{exp}) = \frac{|P_{pra} \cup P_{exp}| - |P_{pra} \cap P_{exp}|}{|P_{pra} \cup P_{exp}|}, \quad (5)$$

where I_{exp} is the synthesized semantic pattern with predicted class. $P_{pra} \cap P_{exp}$ means the numbers of pixels where the pixel value of P_{pra} and P_{exp} both equal to 1.

Self-Verification: With the derived inconsistency metric, we propose our specific detection methodology which contains the self-verification stage. The entire process of our method is described in Fig. 3. For each input image, we apply CAM to locate the source location of the biggest model activations. Then we crop the image to obtain the patterns with maximum activations. In the step of semantic test, we calculate the consistency between I_{pra} and I_{exp} . Once the inconsistency value is higher than a predefined threshold, we consider an adversarial input detected. With above steps, we can detect the image physical adversarial attack through self-verification stage during CNN inference process.

5 AUDIO PHYSICAL ADVERSARIAL ATTACK DETECTION

In this section, we will introduce the detailed detection flow for audio physical adversarial attacks.

Inconsistency Derivation: We leverage the **prediction activation inconsistency** to detect audio physical adversarial attacks since the original input audio will loss semantics after the Mel-frequency Cepstral Coefficient (MFCC) conversion. More specifically, we measure the activation magnitude distribution inconsistency between the practical input and the synthesized data with

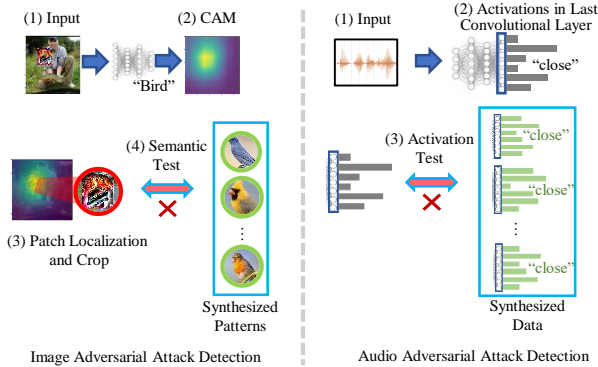


Figure 3: Detection Process for Image and Audio Physical Adversarial Attacks

the same prediction class. We adopt a popular similarity evaluation method - Pearson Correlation Coefficient (PCC) [4] and the inconsistency metric is defined as:

$$D(f_{pre}f_{exp})=1-PCC(f_{pre}f_{exp})=1-\frac{E[(f_{pre}-\mu_{pre})(f_{exp}-\mu_{exp})]}{\sigma_{pra}\sigma_{exp}}, \quad (6)$$

where I_{pre} and I_{exp} represent the activations in the last convolutional layer for both practical input and synthesized input. μ_a and μ_o denote the mean values of f_{pre} and f_{exp} , σ_{pra} and σ_{exp} are the standard derivations, and E means the overall expectation.

Self-Verification: With derived inconsistency metric, we further apply self-verification stage to CNN for the audio physical adversarial attack. The detection flow is described as following: We first obtain activations in the last convolutional layer for every possible input word by testing CNN with a standard dataset. Then we calculate the inconsistency value $D(I_{pra}, I_{exp})$. If the model is attacked by the audio adversarial attack, $D(I_{pra}, I_{exp})$ will exceed a pre-defined threshold. According to our preliminary experiments which are tested with various attacks, $D(I_{pra}, I_{exp})$ of an adversarial input is usually larger than 0.18 while a natural input’s $D(I_{pra}, I_{exp})$ is usually smaller than 0.1. Therefore, there exists a large range for the threshold to distinguish the natural and the adversarial input audios, which can benefit our accurate detection.

6 EXPERIMENT AND EVALUATION

In this section, we evaluate our method’s effectiveness in terms of image and audio physical adversarial attacks. For physical adversarial attack in image scenarios, we test our detection method’s performance on Inception-V3 [23], VGG-16 [21], and ResNet-18 [14] using ImageNet dataset [9]. For audio scenarios, we use Command Classification Model [17] on Google Voice Command dataset [17].

6.1 CNN Image Physical Adversarial Attack Detection Evaluation

Our detection method is mainly evaluated for adversarial patch attacks. The adversarial patches are generated by using Inception-V3 as the base model. The generated patches with high transferability are utilized to attack three models: Inception-V3 itself and two other models, namely VGG-16 and ResNet-18. Then we apply our detection method on the attacks for three models and test their detection success rates. The baseline method is *Blind*, which is one state-of-the-art detection method [13]. And the threshold for inconsistency is set as 0.46. Table 1 shows the overall detection

Table 1: Image Adversarial Attack Detection Evaluation

Model/Method	Inception-V3		VGG-16		ResNet-18	
	Blind*	Ours	Blind*	Ours	Blind*	Ours
Detection Succ. Rate	88%	91%	89%	90%	85%	89%

*:Blind [13]

Table 2: Audio Adversarial Attack Detection Evaluation

Method	FGSM	BIM	CW	Genetic
Dependency Detection	91%	89%	90%	88%
Multiversion Detection	81%	73%	79%	68%
Ours	95%	94%	94%	92%

performance. *Blind* achieves an average rate of 87% success for detection while *DoPa* demonstrate an average 90% detection successful rate. On all three models, *DoPa* consistently shows higher detection success rate than [13]. By the above comparison, we show that our detection method has better detection performance than *Blind* w.r.t detection effectiveness.

6.2 CNN Audio Physical Adversarial Attack Detection Evaluation

Since there exists a large range for the inconsistency threshold to distinguish the natural and the adversarial audio, we leverage the grid search to find the best one and set as 0.11 in this experiment. For comparison, we re-implement another two state-of-the-art detection methods: *Dependency Detection* [26] and *Multiversion* [27]. Four methods [1, 6, 12, 16] are used as attacking methods to prove the generality of our detection method. Table 2 shows the overall performance comparison results.

DoPa can always achieve more than 92% detection success rate for all types of audio physical adversarial attacks. By contrast, *Dependency Detection* achieves 89% detection success rate in average while *Multiversion Detection* only has average 74%. Therefore, *DoPa* demonstrates a best detection accuracy.

7 CONCLUSION

In this paper, we propose a CNN detection methodology for physical adversarial attacks for both image and audio recognition applications. Leveraging the comprehensive CNN vulnerability analysis and two novel CNN inconsistency metrics, our method can effectively detect both image and audio physical adversarial attacks with average 90% and 92% detection successful rates.

REFERENCES

- [1] M. Alzantot and *et al.* 2018. Did You Hear that? Adversarial Examples Against Automatic Speech Recognition. *arXiv preprint arXiv:1801.00554* (2018).
- [2] C. Ayres and *et al.* 2008. Measuring Fiber Alignment in Electrospun Scaffolds: A User’s Guide to the 2D Fast Fourier Transform Approach. *Journal of Biomaterials Science, Polymer Edition* 19, 5 (2008), 603–621.
- [3] Adith B and *et al.* 2019. Simple physical adversarial examples against end-to-end autonomous driving models. *arXiv preprint arXiv:1903.05157* (2019).
- [4] J. Benesty and *et al.* 2009. Pearson Correlation Coefficient. In *Noise reduction in speech processing*. Springer, 1–4.
- [5] T. Brown and *et al.* 2017. Adversarial Patch. *arXiv preprint arXiv:1712.09665* (2017).
- [6] N. Carlini and *et al.* 2017. Towards Evaluating the Robustness of Neural Networks. In *Proc. of SP*. 39–57.
- [7] C. Chiu and *et al.* 2018. State-of-the-art Speech Recognition with Sequence-to-sequence Models. In *Proc. of ICASSP*. 4774–4778.
- [8] J. Chorowski and *et al.* 2015. Attention-based Models for Speech Recognition. In *Proc. of NIPS*. 577–585.
- [9] J. Deng and *et al.* 2009. Imagenet: A large-scale Hierarchical Image Database. In *Proc. of CVPR*. 248–255.
- [10] D. Erhan and *et al.* 2009. Visualizing Higher-layer Features of A Deep Network. *University of Montreal* 1341, 3 (2009), 1.

- [11] K. Eykholt and *et al.* 2017. Robust Physical-world Attacks on Deep Learning Models. *arXiv preprint arXiv:1707.08945* (2017).
- [12] I. Goodfellow and *et al.* 2014. Explaining and Harnessing Adversarial Examples. *arXiv preprint arXiv:1412.6572* (2014).
- [13] J. Hayes. 2018. On Visible Adversarial Perturbations & Digital Watermarking. In *Proc. of CVPR Workshops*. 1597–1604.
- [14] K. He and *et al.* 2015. Deep Residual Learning for Image Recognition. In *Proc. of CVPR*. 770–778.
- [15] V. James. 2018. Google is making it easier than ever to give any app the power of object recognition. <https://www.theverge.com/2017/6/15/15807096/google-mobile-ai-mobilenets-neural-networks>
- [16] A. Kurakin and *et al.* 2016. Adversarial Examples in the Physical World. *arXiv preprint arXiv:1607.02533* (2016).
- [17] S. Morgan and *et al.* 2001. Speech Command Input Recognition System for Interactive Computer Display with Term Weighting Means Used in Interpreting Potential Commands from Relevant Speech Terms. US Patent 6,192,343.
- [18] M. Naseer and *et al.* 2019. Local Gradients Smoothing: Defense against localized adversarial attacks. In *Proc. of WACV*. 1300–1307.
- [19] S. Niwattanakul and *et al.* 2013. Using of Jaccard Coefficient for Keywords similarity. In *Proc. of IMECS*, Vol. 1. 380–384.
- [20] M. Osadchy and *et al.* 2017. No Bot Expects the DeepCAPTCHA! Introducing Immutable Adversarial Examples, With Applications to CAPTCHA Generation. *IEEE Transactions on Information Forensics and Security* 12, 11 (2017), 2640–2653.
- [21] K. Simonyan and *et al.* 2014. Very Deep Convolutional Networks for Large-scale Image Recognition. *arXiv preprint arXiv:1409.1556* (2014).
- [22] C. Szegedy and *et al.* 2013. Intriguing Properties of Neural Networks. *arXiv preprint arXiv:1312.6199* (2013).
- [23] C. Szegedy and *et al.* 2015. Going Deeper with Convolutions. In *Proc. of CVPR*. 1–9.
- [24] F. Wang and *et al.* 2017. Residual Attention Network for Image Classification. In *Proc. of CVPR*. 3156–3164.
- [25] H. Yakura and *et al.* 2018. Robust Audio Adversarial Example for A Physical Attack. *arXiv preprint arXiv:1810.11793* (2018).
- [26] Z. Yang and *et al.* 2018. Characterizing Audio Adversarial Examples Using Temporal Dependency. *arXiv preprint arXiv:1809.10875* (2018).
- [27] Q. Zeng and *et al.* 2018. A Multiversion Programming Inspired Approach to Detecting Audio Adversarial Examples. *arXiv preprint arXiv:1812.10199* (2018).
- [28] B. Zhou and *et al.* 2016. Learning Deep Features for Discriminative Localization. In *Proc. of CVPR*. 2921–2929.
- [29] B. Zoph and *et al.* 2018. Learning Transferable Architectures for Scalable Image Recognition. In *Proc. of CVPR*. 8697–8710.